




## Microstructural, mechanical, and corrosion properties of S355J2 structural steels joined by MIG welding

Uğur Çaligülü<sup>1</sup> , Cihan Özorak<sup>2\*</sup> , Afif Daniş<sup>1</sup> 

<sup>1</sup>Firat University, Faculty of Technology, Department of Metallurgy and Materials Engineering, Elazığ-Turkey

<sup>2</sup>Kastamonu University, School of Civil Aviation, Department of Aircraft Maintenance and Repair, Kastamonu-Turkey

### Article Info

Research article  
Received: 24/09/2024  
Revision: 25/10/2024  
Accepted: 02/11/2024

### Keywords

S355J2 Structural Steel  
MIG Welding  
Corrosion  
Microstructure  
Mechanical Properties

### Makale Bilgisi

Araştırma makalesi  
Başvuru: 24/09/2024  
Düzelme: 25/10/2024  
Kabul: 02/11/2024

### Anahtar Kelimeler

S355J2 Yapısal Çelik  
MIG Kaynağı  
Korozyon  
Mikroyapı  
Mekanik Özellikler

### Graphical/Tabular Abstract (Grafik Özet)

In this study, the microstructural, mechanical, and corrosion properties of S355J2 structural steels welded by metal inert gas (MIG) welding method were investigated. Single surface and double surface welded structures were formed by MIG welding method using 2 different amperage values (200A, and 260A).

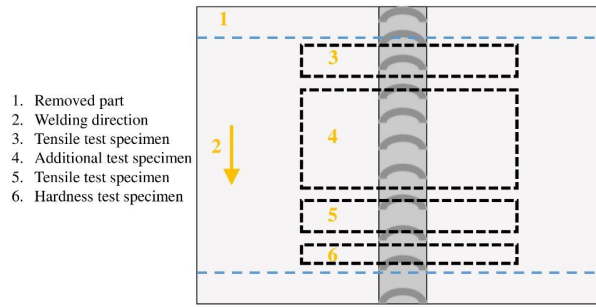


Figure A: Butt-to-face joint test sample preparation areas according to TS EN ISO 15614-1 standard/ Şekil A: TS EN ISO 15614-1 standardına göre uç uca birleştirme deney numunesi hazırlama alanları

### Highlights (Önemli noktalar)

- The gas metal arc welding capability of S355J2 structural steel, which is widely preferred in the oil and offshore sector, was investigated according to EN ISO 15614-1 standard. / Petrol ve açık deniz sektöründe yaygın olarak tercih edilen S355J2 yapı çeliğinin gaz altı kaynak kabiliyeti EN ISO 15614-1 standardına göre araştırılmıştır.
- The microstructure images were examined under an optical microscope, it was observed that the material had a ferritic and pearlitic structure. In addition, it was observed that the welding current increased and the grain size increased in double-sided welding. / Mikro yapı görüntüleri optik mikroskop altında incelendiğinde, malzemenin ferritik ve perlitik yapıya sahip olduğu gözlemlendi. Ayrıca, kaynak akımının arttığı ve çift taraflı kaynakta tane boyutunun arttığı tespit edilmiştir.
- Corrosion test results showed that the welded joint welded at 260A welding current and double-sided was more resistant to corrosion in 1M HCl solution than other samples. / Korozyon testi sonuçları, 260A kaynak akımında ve çift taraflı olarak kaynaklanan kaynaklı birleştirmenin, 1M HCl çözeltisinde diğer numunelere göre korozyona karşı daha dayanıklı olduğunu göstermiştir.

**Aim (Amaç):** In this study, the gas welding capability of S355J2 structural steel, which is widely preferred in the oil and offshore sectors, was investigated. / Bu çalışmada petrol ve açık deniz sektöründe yaygın olarak tercih edilen S355J2 yapı çeliğinin gaz altı kaynak kabiliyeti incelenmiştir.

**Originality (Özgünlük):** It was investigated whether the strength changed as a result of changing the welding method and amperage value of the welding process. / Kaynak işleminin kaynak metodu ve amper değerinin değişmesi sonucu dayanımın değişip değişmediği araştırılmıştır.

**Results (Bulgular):** Tensile test results showed that there was an increase in both yield strength and tensile strength in double-sided welding and 260A welding current. / Çekme testi sonuçları, çift taraflı kaynak ve 260A kaynak akımında hem akma dayanımında hem de çekme dayanımında artış olduğunu göstermiştir.

**Conclusion (Sonuç):** Considering all test results, it was seen that the most suitable welding parameters were 260A and double-sided welding sample. / Tüm test sonuçları göz önüne alındığında en uygun kaynak parametrelerinin 260A ve çift taraflı kaynak numunesi olduğu görülmüştür.



## Microstructural, mechanical, and corrosion properties of S355J2 structural steels joined by MIG welding

Uğur Çaligülü<sup>1</sup>, Cihan Özorak<sup>2\*</sup>, Afif Daniş<sup>1</sup>

<sup>1</sup>Firat University, Faculty of Technology, Department of Metallurgy and Materials Engineering, Elazığ-Turkey

<sup>2</sup>Kastamonu University, School of Civil Aviation, Department of Aircraft Maintenance and Repair, Kastamonu-Turkey

### Article Info

Research article  
Received: 24/09/2024  
Revision: 25/10/2024  
Accepted: 02/11/2024

### Keywords

S355J2 Structural Steel  
MIG Welding  
Corrosion  
Microstructure  
Mechanical Properties

### Abstract

In this study, the microstructural, mechanical, and corrosion properties of S355J2 structural steels welded by metal inert gas (MIG) welding method were investigated. Single surface and double surface welded structures were formed by MIG welding method using 2 different amperage values (200A, and 260A). The microhardness, tensile strength, corrosion and microstructure properties of the welded specimens were investigated. The structural and mechanical effects of different current values used on the material were analysed. Microstructure investigations show that fine grained structures start to coarsen and grain boundaries start to decrease due to welding heat input in the HAZ region. The highest hardness value was measured in the welded joint at 260A value in single surface welding due to rapid cooling and rapid solidification. Increases in yield strength and tensile strength were determined with increasing welding current and in the double-sided welding procedure. In the potentiodynamic corrosion test carried out in HCl solution, it was determined that the double-sided welded joint at 260A welding amperage and the double-sided welded joint at 260A was the most resistant to corrosion among the samples subjected to corrosion tests.

## MIG kaynağı ile birleştirilen S355J2 yapısal çeliklerinin mikro yapısal, mekanik ve korozyon özellikleri

### Makale Bilgisi

Araştırma makalesi  
Başvuru: 24/09/2024  
Düzeltilme: 25/10/2024  
Kabul: 02/11/2024

### Anahtar Kelimeler

S355J2 Yapısal Çelik  
MIG Kaynağı  
Korozyon  
Mikroyapı  
Mekanik Özellikler

### Öz

Bu çalışmada, metal inert gaz (MIG) kaynak yöntemi ile kaynaklanan S355J2 yapı çeliklerinin mikro yapısal, mekanik ve korozyon özellikleri incelenmiştir. MIG kaynak yöntemi ile 2 farklı amper değeri (200A ve 260A) kullanılarak tek yüzey ve çift yüzey kaynaklı yapılar oluşturulmuştur. Kaynaklanan numunelerin mikro sertlik, çekme dayanımı, korozyon ve mikro yapı özellikleri incelenmiştir. Kullanılan farklı akım değerlerinin malzeme üzerindeki yapısal ve mekanik etkileri analiz edilmiştir. Mikro yapı incelemeleri, ince taneli yapıların HAZ bölgesinde kaynak ısısı girdisi nedeniyle kabalaşmaya başladığını ve tane sınırlarının azalmaya başladığını göstermektedir. En yüksek sertlik değeri, tek yüzey kaynakta hızlı soğuma ve hızlı katılma nedeniyle kaynaklı bağlantıda 260A değerinde ölçülmüştür. Kaynak akımının artırılmasıyla ve çift taraflı kaynak işleminde akma dayanımı ve çekme dayanımında artışlar belirlenmiştir. HCl çözeltisinde yapılan potansiyodinamik korozyon deneyinde, 260A kaynak amperinde çift taraflı kaynaklı birleştirmenin, korozyon deneyine tabi tutulan numuneler arasında ise çift taraflı kaynaklı birleştirmenin korozyona en dayanıklı olduğu belirlenmiştir.

## 1. INTRODUCTION (GİRİŞ)

Structural steels are generally used in bridges, industrial construction, breakwaters, shipbuilding, oil and offshore gas platforms and railways. The main properties required in structural steels are high yield strength, tensile strength, elongation and easy

weldability. The reasons for the significant use of structural steel in the mentioned areas today are its easy accessibility, economic suitability, high yield and tensile strength [1]. Since they do not contain alloying elements, their properties are controlled by their carbon percentage. The increase in carbon content increases the yield and tensile strengths and

hardenability, and decreases the ductility and toughness values. Structural steels, which are steels with low carbon content, deform more than steels with high carbon content. They have low hardenability values due to their unalloyed and low carbon content, so they cannot be hardened as a result of heat treatment. Only softening and stress relieving processes can be applied as heat treatment [2]. For this reason, the welding capabilities of S355J2 structural steel, one of the most widely used materials in the world, were investigated according to EN ISO 15614-1 standard. S355J2 structural steel has low carbon content, pearlitic+ferritic fine grain structure and high yield and tensile values. Therefore, it has encouraged to investigate different welded joining methods for the material to work without losing its values and properties after the welding process.

Metal inert gas (MIG) welding method is a joining process that is used to increase the welding arc stability by using shielding inert gas; the arc between the electrode and work pieces fed into the welding zone melts the metallic material. It is very suitable for use in semi-/full automatic manufacturing system. This allows us to save time and create fast delivery times [3]. Since smaller diameter electrodes are used compared to arc welding, it has high current density and high metal deposition rate in the same current range. Since slag is not released, there is no slag cleaning work after each pass made with covered electrodes and the welding quality is improved since there is no possibility of slag residue in the weld [4,5].

When examined in the literature, it has been observed that structural steels are used in scientific studies to find the most suitable welded manufacturing methods by using many welded manufacturing methods and welding variables in order to maximise the mechanical properties of the material. Ertürk et al. [6] stated that for structural steels, a carbon content less than  $C \leq 0.22$  reduces the possibility of capillary cracks in the weld seam, and the amount of martensite formed in the weld seam at the time of welding should not exceed 30% by reducing the amount of carbon in the content. Eleman [7] investigated the effects of new and old generation MIG-MAG gas metal arc welding machines on welding. It has been observed that the new generation machines have better penetration, spatter problem occurs much less, while root

formation occurs in the welding process with the traditional welding machine, it has been observed that the rupture occurs on the weld seam. The microstructure and mechanical behavior of S355J2 steel base metal, welded joints, and repair welded joints were examined by Yu et al. [8]. According to their testing, the microhardness of repair welded joints drops by roughly 20 HV as the heat affected zone and weld metal's grain size increase. When taking into account the cyclic loading behavior, the repair welded joints showed a higher degree of softening than the welded joints and exhibited continuous softening. The impact of repair welding on the microstructure, mechanical characteristics, and fatigue characteristics of S355J2 steel T-joints in orthotropic bridge decks was examined by Zhao et al. [9]. According to the test results, the heat-affected coarse zone's increased grain size resulted in a about 30 HV decrease in the hardness of the connection.

In this study, the gas metal arc welding capability of S355J2 structural steel, which is widely preferred in the oil and offshore sector, was investigated according to EN ISO 15614-1 standard. For this reason, S355J2 structural steel was welded by MIG gas metal arc welding method using 2 different amperage values; 100% argon shielding gas, SG2 welding wire and constant welding speed as single surface and double surface welding and the microstructure, mechanical and corrosion properties of the welded joint were examined in detail.

## **2. EXPERIMENTAL STUDIES (DENEYSEL ÇALIŞMALAR)**

In the study, S355J2 structural steel was commercially available in dimensions of 100 mm x 100 mm x 5 mm. Commercial 1.2 mm gas wire and 100% argon gas was used as shielding gas. Since the wall thickness of the S355J2 plates used was 5 mm, no pre-annealing process was performed. The materials to be welded were joined by MIG gas metal arc welding method using 200A and 260A at different amperage values as S355J2-S355J2 plate pairs, keeping the shielding gas, welding wire and welding speed constant. Single and double sided surfaces of S355J2 plates were welded using MIG method. The chemical composition and mechanical properties of the S355J2 material used in Table 1 are given in Table 2.

**Table 1.** Chemical composition of S355J2 structural steel (S355J2 yapısal çeliğin kimyasal bileşimi)

Grade	Chemical composition (wt.%)						
	C	Si	Mn	P	S	Cu	Fe
S355J2	0,22	0,55	1,6	0,025	0,025	0,55	Balance

**Table 2.** Mechanical properties of S355J2 structural steel (S355J2 yapısal çeliğin mekanik özellikleri)

Grade	Yield strength (N/mm <sup>2</sup> )	Tensile strength (N/mm <sup>2</sup> )	Elongation (%)	Impact energy (J)	
				- 20 °C	+ 20 °C
S355J2	355	510	17	27	40

During the welding process, a Lincoln PF46 type welding machine was used. The welding process was carried out at 200A and 260A amperes, 24-27V welding voltage and argon protective gas atmosphere. The prepared single and double sided surface welded specimens were subjected to SEM-EDX, XRD, tensile, hardness, corrosion and tensile,

hardness and grain structure tests and samples were cut from the welded sections to examine the grain structure under optical microscope. The samples prepared for metallographic examination were cut from the welded materials according to TS EN ISO 15614-1 standards from the areas specified in Figure 1 for the tests.

1. Removed part
2. Welding direction
3. Tensile test specimen
4. Additional test specimen
5. Tensile test specimen
6. Hardness test specimen

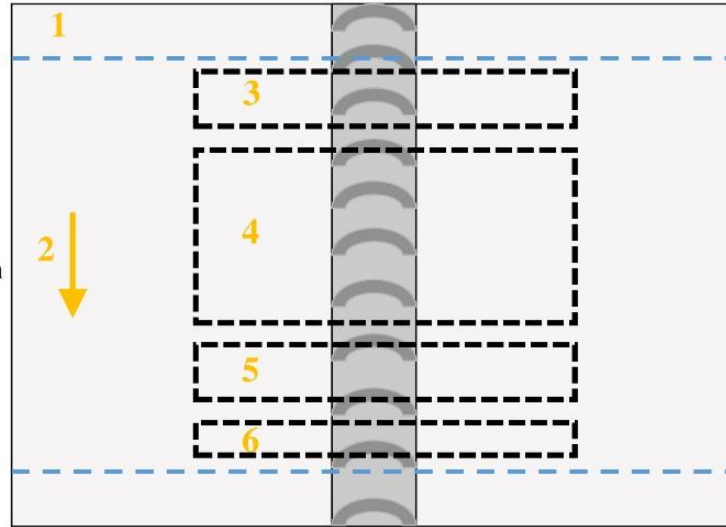


**Figure 1.** Butt-to-face joint test sample preparation areas according to TS EN ISO 15614-1 standard (TS EN ISO 15614-1 standardına göre uç uca birleştirme deney numunesi hazırlama alanları)

Welded samples were polished after surface sanding and etched in nital solution. Microhardness measurements were carried out using an AOB brand microhardness device. These measurements were made from a total of 20 different places under a load of 300 g, at 1 mm intervals and within a period of 20 seconds. A general evaluation was made by taking the average of these measurements. Tensile tests were carried out on a Shimadzu brand limited tensile device with a load of 50 kN, at a tensile speed of 3 mm/minute and in accordance with the TSE 138 EN 10002-1 standard. The Reference 3000 potentiostat/galvanostat/ZRA instrument was utilized to evaluate the samples for corrosion. The samples were ultrasonically cleaned for 45 minutes

at 35 °C with acetone, followed by 15 minutes at 35 °C with distilled water and 15 minutes at 60 °C with ethanol, and finally dried at 60 °C before beginning the corrosion study. The cleaned samples' open circuit potentials were measured for around fifteen minutes in a 1M HCl solution. The graphite electrode used as counter electrode. Reference electrode were represented by the Ag/AgCl electrode. Potentiodynamic polarization experiments and electrochemical impedance spectroscopy (EIS) measurements were performed on all samples. For every sample, three experiments were run. Samples were cleaned, a fresh solution was utilized, and the outcomes were averaged for each experiment. Microstructure analysis of the

samples and evaluation of the broken surfaces were made with a Zeiss brand scanning electron microscope and a Nikon brand optical microscope.

### 3. RESULTS AND DISCUSSION (SONUÇLAR VE TARTIŞMA)

The optical photographs of the specimens welded with single/double sided surface using 200A welding current are shown in Figure 2 and the optical photographs of the specimens welded with 260A welding current are shown in Figure 3. In Figure 2a and Figure 3a, single sided surface welding was performed, while in Figure 2b and Figure 3b, double sided surface welding was performed. For each specimen, the welded joint consists of three zones: weld zone, HAZ and base metal. Porous (cellular) and dendritic solidification was observed in the specimens in the direction

opposite to the heat flow starting from the melting line towards the centre of the melt pool. However, planar solidification was observed at the interface in contrast to dendritic solidification. This can be explained by the high temperature gradient ( $\Delta T$ ) and low solidification rate ( $V$ ) at the interface. Dendritic solidification is also observed when the  $\Delta T/V$  ratio is low. From the weld zone to the base metal, a coarse grain zone (HAZ) and then a fine grain zone (base metal) were formed [10–12]. In the transition from single sided surface to double sided surface and from 200A to 260A, coarsening of the grains in the structure occurred due to the increase in heat input. In their study on the mechanical and microstructure of the welded structure of a low carbon steel, Eroglu et al. [13] reported that the grain size increases in the weld zone and HAZ with increasing heat input.

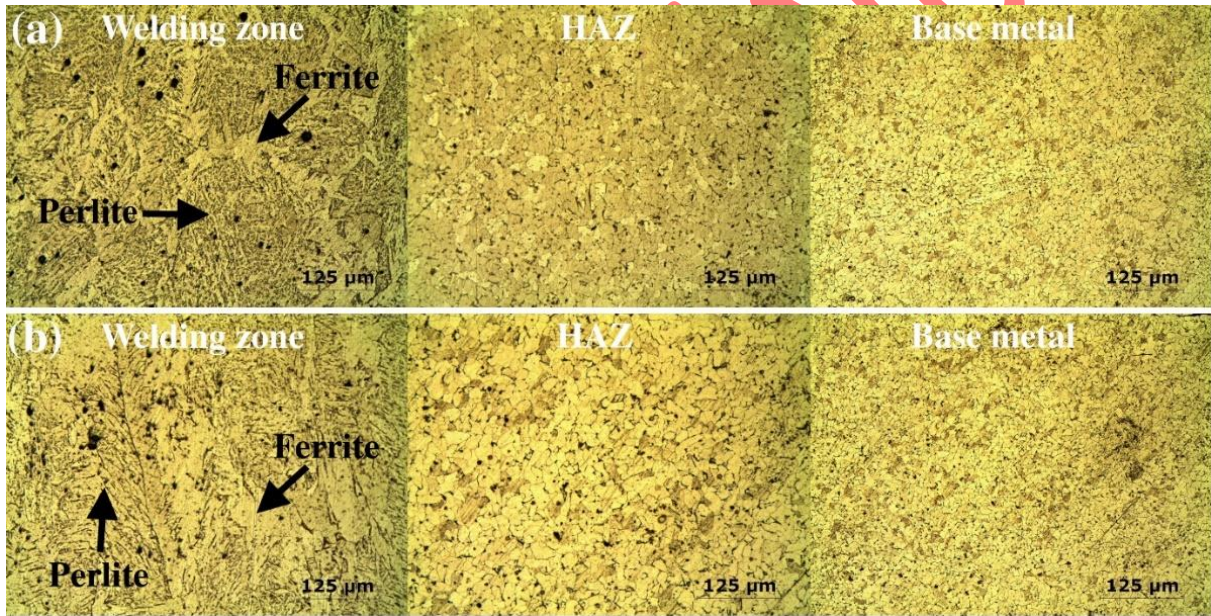


**Figure 2.** Optical photographs of the specimens welded at 200A welding current: (a) single sided surface and (b) double sided surface (200A kaynak akımında kaynaklanmış numunelerin optik fotoğrafları: (a) tek taraflı yüzey ve (b) çift taraflı yüzey)

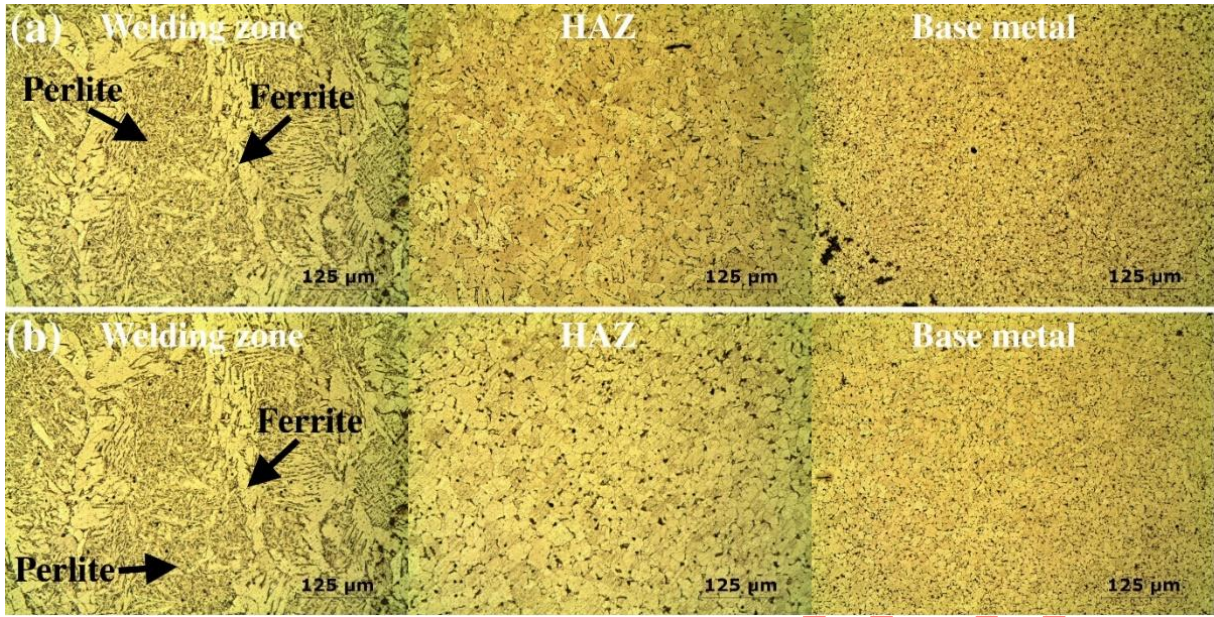


**Figure 3.** Optical photographs of the specimens welded at 260A welding current: (a) single sided surface and (b) double sided surface (260A kaynak akımında kaynaklanmış numunelerin optik fotoğrafları: (a) tek taraflı yüzey ve (b) çift taraflı yüzey)

Figure 4 shows the SEM-EDS analysis of the weld zone of the specimen welded on both sides at 260A welding current. EDS analysis of the structure consists of 0.21% C, 0.53% Si, 1.51% Mn, and 97.75% Fe. This chemical composition is consistent

with the chemical composition of the base metal given in the experimental studies section. In addition, the absence of any oxygen in the structure indicates that the weld zone is effectively protected by argon gas.

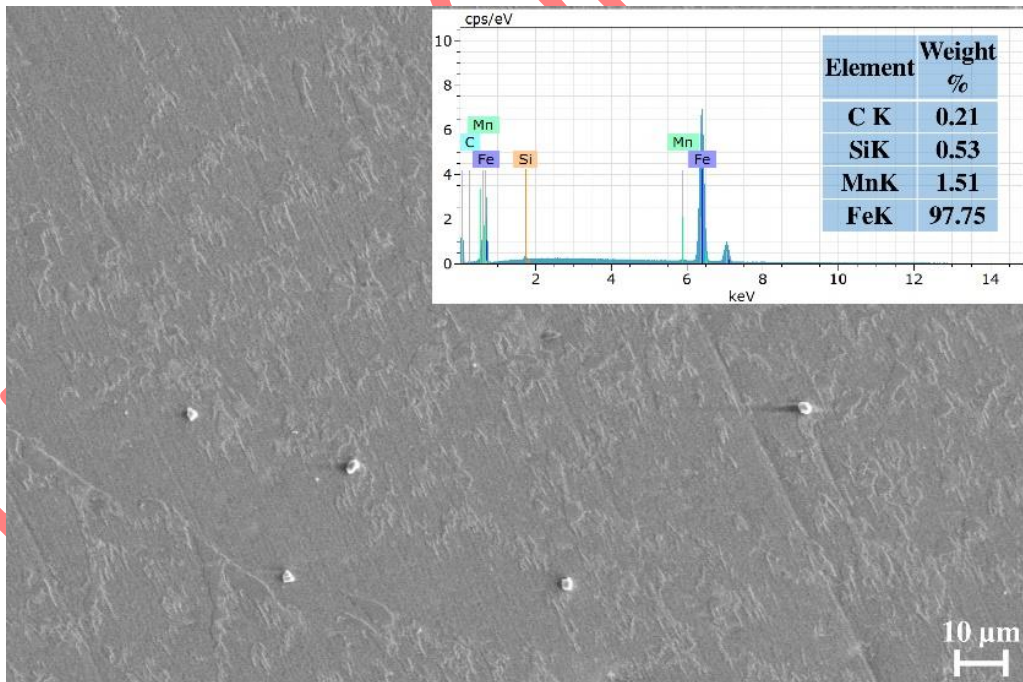


**Figure 4.** SEM-EDS analysis of the weld zone at 260A welding current and double-sided welded specimen (260A kaynak akımında kaynak bölgesinin ve çift taraflı kaynaklı numunenin SEM-EDS analizi)

The hardness graph of the samples is given in Figure 5. As a result of the tests, hardness values were generally high in the area where the weld seam was located due to rapid cooling and solidification in the weld zone. The highest hardness value was 219.9

HV on 260A single sided surface and the lowest was 132.5 HV on 200A double sided surface. The average hardness value was 180.49 HV for 260A single sided surface welded material and the lowest value was 160 HV for 200A single sided surface

welded material. The hardness value in the weld seam and HAZ region increased with increasing amperage value. It is thought to be caused by grain growth and dendritic solidification as a result of sudden cooling and sudden solidification with heat input during the welding process in the area of the weld seam. The fact that the hardness in the welding region is greater than the HAZ can be explained as

the high heat in the welding region is trapped in the HAZ region and reduces the hardness in this region [14-15]. Therefore, the reduced hardness in the HAZ may be attributed to the occurrence of grain development and the presence of ferrite phase in this area, as previously documented by other researchers [15-16].

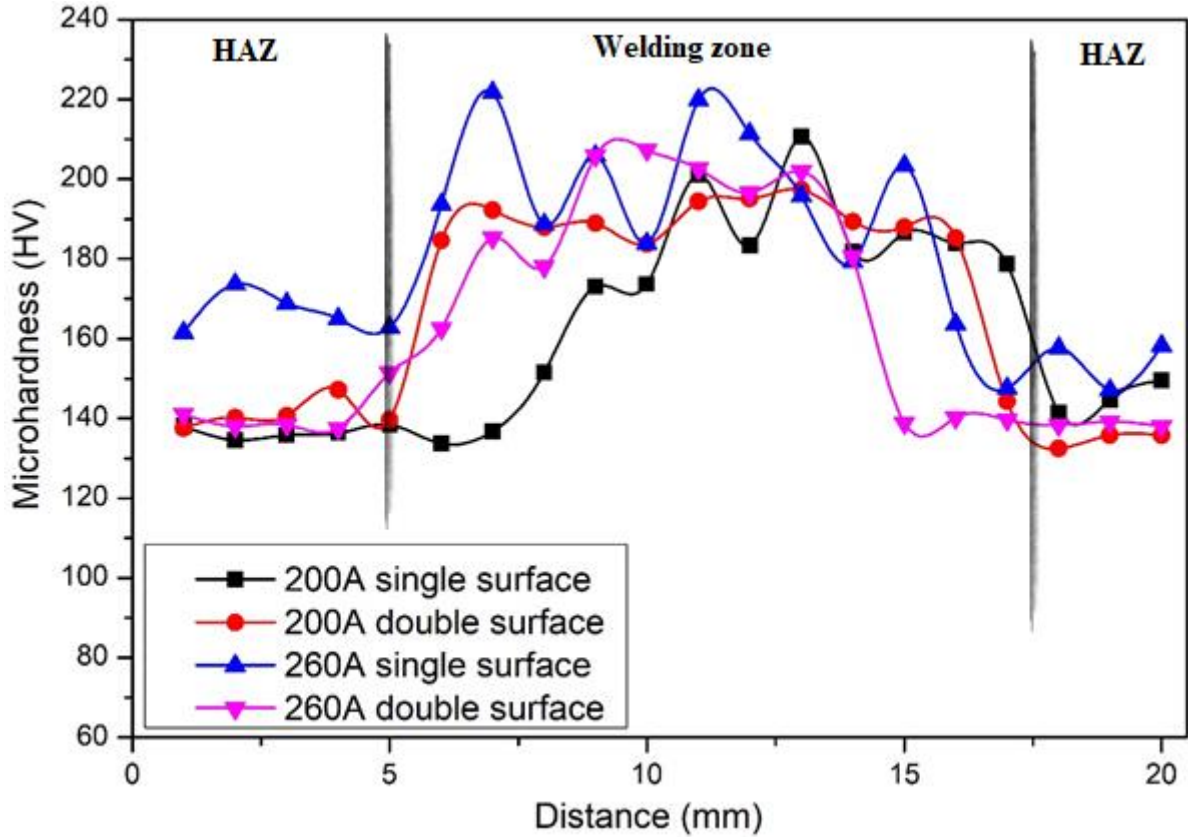
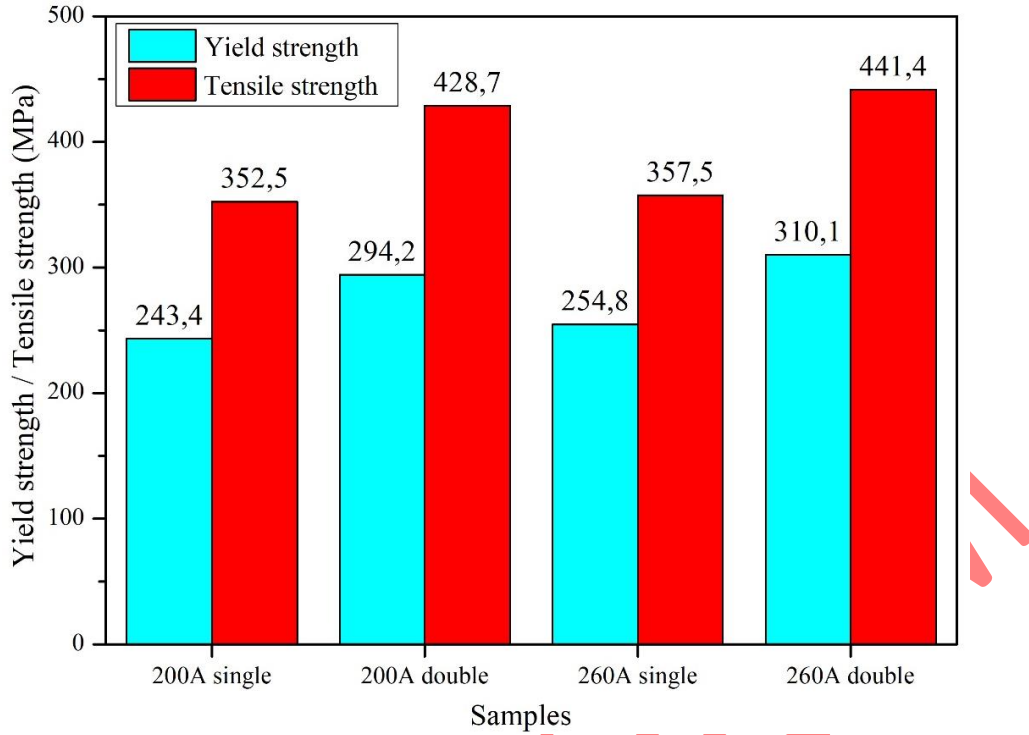


Figure 5. Hardness graph of the samples (Numunelerin sertlik grafiği)

The yield strength and tensile strength graphs of the specimens are given in Figure 6. When the data obtained are analysed, it is observed that the yield and tensile strength of the material is low in single sided surface welded specimens and high in double sided surface welded specimens. In addition, as the welding current increased, the yield strength and tensile strength of the welded specimens increased. More penetration was achieved both in double-sided welding and with increasing welding current. While the ruptures occurred at the weld area in the single-sided welded specimens, they occurred at the neck in the double-sided welded specimens. Figure

7 shows the occurrence of single and double sided welds in different regions in 260A. In single-sided welding, fracture occurred due to insufficient strength of the welded area. No necking was observed in this fracture. However, after double-sided welding, no fracture occurred in the welded area with higher strength, necking and subsequent fracture occurred in the base metal. 17 Tuncel and Aydın [18] studied the effect of welding type and pulse frequency on the tensile properties of Nd:YAG laser welded DP600 steel sheets. Double-sided joints have been reported to have significantly higher tensile properties than single-sided joints.



**Figure 6.** Tensile strength and yield strength of specimens (Numunelerin çekme dayanımı ve akma dayanımı)

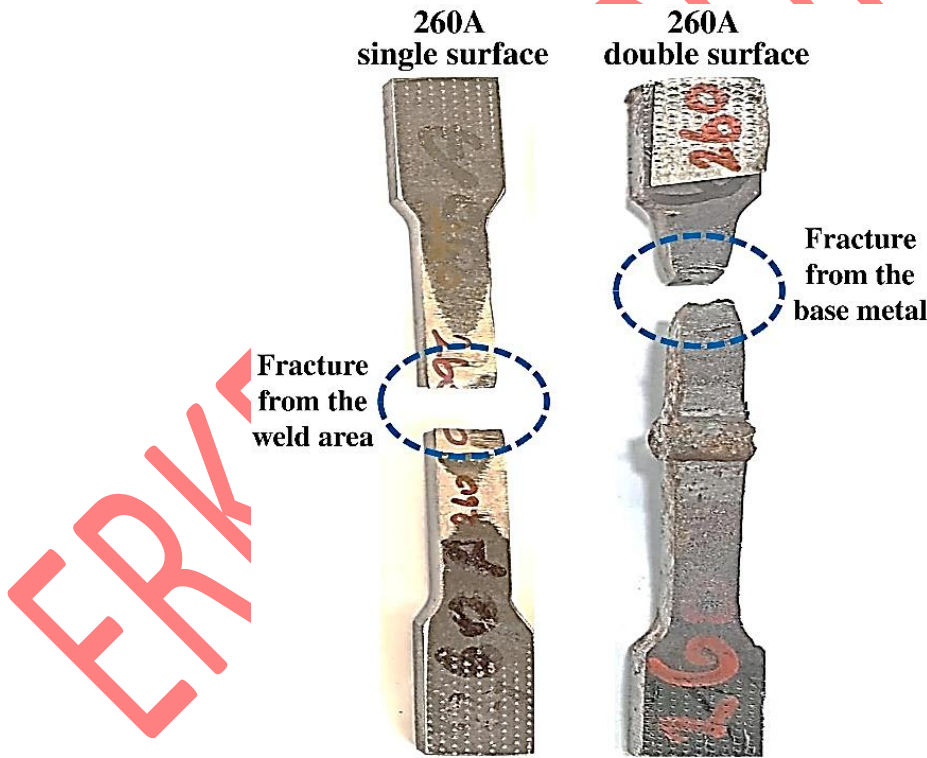


**Figure 7.** Macro view of fracture after tensile testing of single-sided and double-sided welded specimens at 260A welding current (260A kaynak akımında tek taraflı ve çift taraflı kaynaklı numunelerin çekme testinden sonra kırılmanın makro görünümü)

SEM photographs of the fracture surfaces obtained after the tensile test are given in Figure 8. It is seen that the degree of ductile fracture decreases with increasing welding current in single-sided / double-sided welding processes at 200A and 260A welding currents, and the degree of ductility decreases again

in the transition from single-sided welding to double-sided welding at the same ampere value. In the case of ductile fracture, dimple formations are observed. In the case where the degree of ductility decreases, it is seen that the dimples decrease.



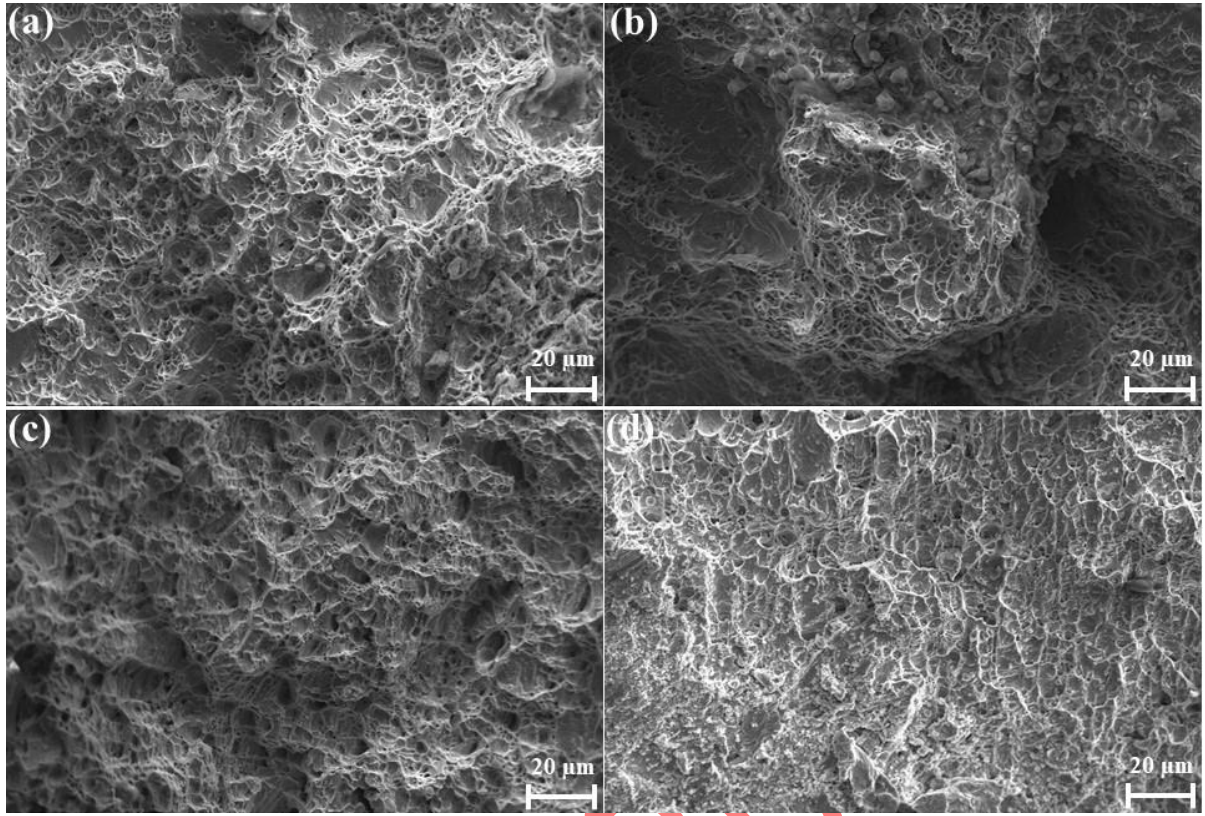


**Figure 8.** Fracture surfaces of the specimens: (a) 200 A single-sided, (b) 260 A single-sided, (c) 200 A double-sided, (d) 260 A double-sided (Numunelerin kırılma yüzeyleri: (a) 200 A tek taraflı, (b) 260 A tek taraflı, (c) 200 A çift taraflı, (d) 260 A çift taraflı)

Potentiodynamic polarization tests were conducted in a 1 M HCl solution to assess the impact of four distinct samples on corrosion. Figure 9 displays the tafel curves acquired for four distinct samples in a 1M HCl environment. The  $i_{corr}$  values were derived using the tafel extrapolation method. Table 3 displays the outcomes of potentiodynamic polarisation studies. The polarization curves depicted in the Figure 9 and the data presented in Table 3 indicate that the corrosion rate of the 260A single surface welded sample is significantly elevated. The current potential curves of the

samples showed a rise in both cathodic and anodic regions, as well as current values, when immersed in a 1 M HCl solution. Borko et al. [19] investigated the corrosion characteristics of the welded junction of S355J2 structural steel. The findings indicated that the base material exhibited the greatest corrosion resistance at a concentration of 0.01M NaCl, while the weld metal demonstrated the lowest corrosion resistance at a concentration of 1M NaCl. According to Tafel results, the lowest corrosion rate was 10.64 mpy on the 260A double sided surface.

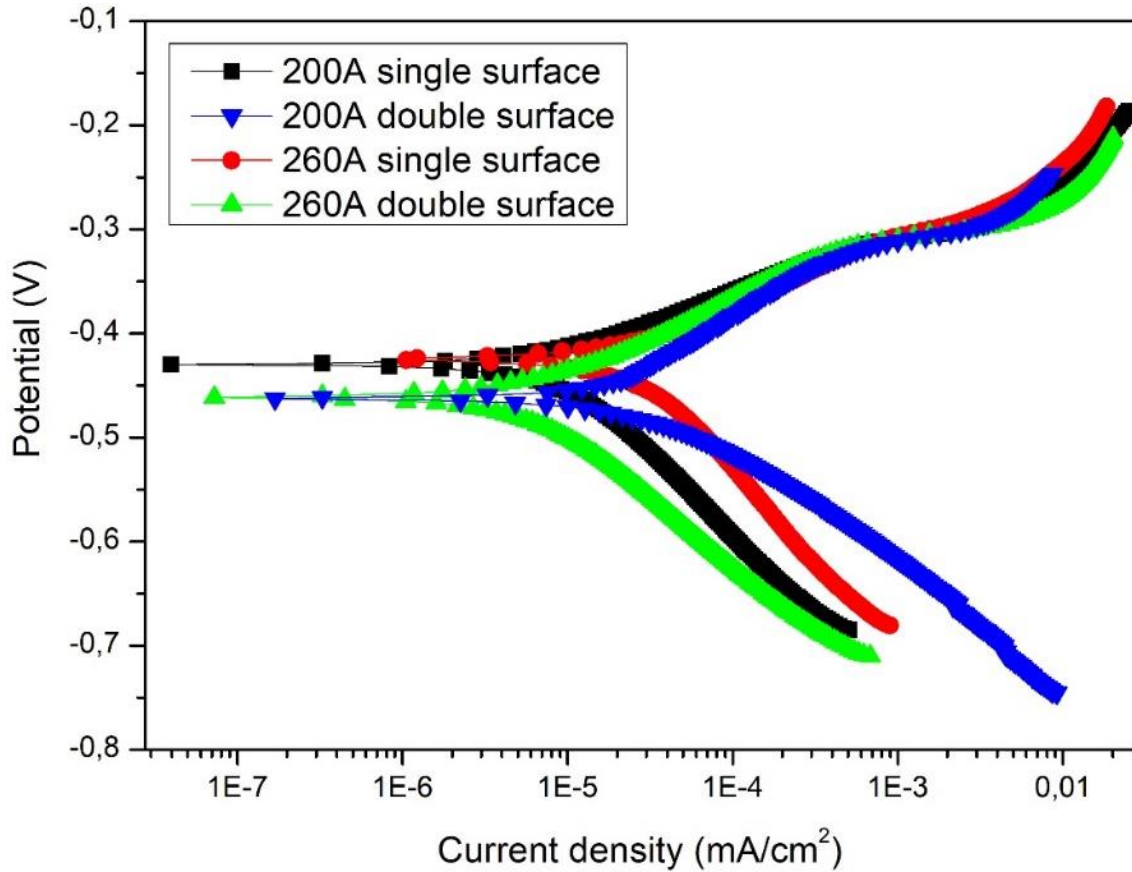


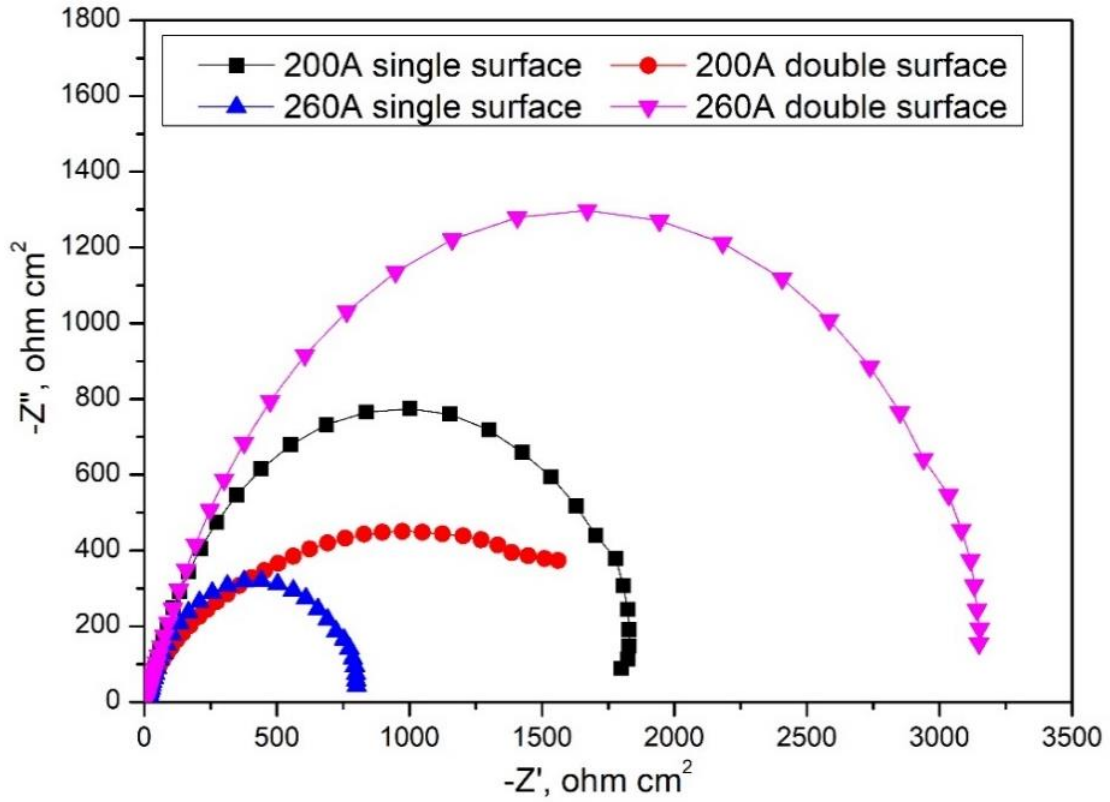
Figure 9. Potentiodynamic polarisation curves (Potansiyodinamik polarizasyon eğrileri)

Table 3. Electrochemical results of the samples (Numunelerin elektrokimyasal sonuçları)

Samples	E <sub>cor</sub> (V)	I <sub>cor</sub> (μAcm <sup>-2</sup> )	β <sub>a</sub> (e <sup>-3</sup> V/decade)	β <sub>c</sub> (e <sup>-3</sup> V/decade)	Corrosion rate (mpy)
200A single sided surface	-0.430	8.60	65.40	144.7	15.71
200A double sided surface	-0.463	16.30	98.90	70.30	29.84
260A single sided surface	-0.425	33.70	87.10	221.5	61.55
260A double sided surface	-0.462	5.82	72.60	129.0	10.64

The Nyquist diagrams of single-sided and double-sided specimens welded at various amperages are presented in Figure 10. The Nyquist diagrams resulting from reactions in solution exhibit a capacitive loop characterized by suppressed

semicircles. The capacitive loop is associated with the load transfer mechanism that regulates the dissolution of the welded specimens in a 1 M HCl solution and the formation of a protective film layer on the surface [20].



**Figure10.** Nyquist diagrams of the specimens (Nyquist diagrams of the specimens)

The system is composed of three components: solution resistance ( $R_s$ ), polarisation resistance ( $R_p$ ), and a stabilized phase element (CPE) coupled in parallel. The  $R_p$  values represent the measured load transfer resistance levels in the given environment. Furthermore, the value of  $R_p$  can be found in Table 4. Table 4 demonstrates that the polarisation resistances fluctuate based on the welding current and the welding type (single and double side). Nyquist diagrams show the capacitive

loop as compressed semicircles. The larger the diameter of the semicircles, the slower the corrosion rate. When Nyquist diagrams were examined, it was seen that the sample with the highest  $r_p$  value was 2633 ohms on the 260A double sided surface. It was determined that this sample had the best corrosion resistance. When comparing Nyquist diagrams with Tafel diagrams, the corrosion rates of the samples showed similar results.

**Table 4.** Impedance spectrum results of samples (Numunelerin empedans spektrum sonuçları)

Properties	Samples			
	200A single sided surface	200A double sided surface	260A single sided surface	260A double sided surface
$R_p$ ( $\Omega$ )	1582	712	679	2633
$R_s$ ( $\Omega$ )	4.775	5.738	7.242	5.078
CPE (F)	$12.87 \times 10^{-6}$	$7.75 \times 10^{-6}$	$30.58 \times 10^{-6}$	$5.64 \times 10^{-6}$

### CONCLUSIONS (SONUÇLAR)

In this study, the microstructure, mechanical and corrosion properties of S355J2 structural steels welded with the MIG welding method at different welding currents and different welding types (single and double-sided) were examined. The results obtained are summarized below:

- When the microstructure images were examined under an optical microscope, it was observed that the material had a ferritic and pearlitic structure. In addition, it was observed that the welding current increased and the grain size increased in double-sided welding.
- According to the microhardness results, the highest hardness value was found to be 219.9 HV in the single-sided welded connection at 260A

welding current, and the lowest hardness value was 132.5 HV in the double-sided welded connection at 200A welding current.

- Tensile test results showed that there was an increase in both yield strength and tensile strength in double-sided welding and 260A welding current. When the fractured surface and SEM images were examined, it was seen that a ductile fracture mechanism occurred. It was determined that the degree of ductility decreased with increasing heat input.

- Corrosion test results showed that when both Tafel and Nquist diagrams were examined, the highest corrosion rate was observed in the 260A single sided surface sample with 61.55 mpy and 679 ohm. The best corrosion resistance was observed in the 260A double sided surface sample with 10.64 mpy and 2633 ohm. Corrosion test results showed that the welded joint welded at 260A welding current and double-sided was more resistant to corrosion in 1M HCl solution than other samples.

#### DECLARATION OF ETHICAL STANDARDS (ETİK STANDARTLARIN BEYANI)

The author of this article declares that the materials and methods they use in their work do not require ethical committee approval and/or legal-specific permission.

Bu makalenin yazarı çalışmalarında kullandıkları materyal ve yöntemlerin etik kurul izni ve/veya yasal-özel bir izin gerektirmediğini beyan ederler.

#### AUTHORS' CONTRIBUTIONS (YAZARLARIN KATKILARI)

**Uğur ÇALIGÜLÜ:** He analyzed the results and performed the writing process.

Deney sonuçlarını analiz etmiş ve maklenin yazım işlemini gerçekleştirmiştir.

**Cihan ÖZORAK:** He conducted the corrosion experiments, analyzed the results and performed the writing process.

Korozyon deneyleri yapmış, sonuçlarını analiz etmiş ve maklenin yazım işlemini gerçekleştirmiştir.

**Afiş DANIŞ:** He conducted the experiments, performed the writing process.

Deneyleri yapmış, maklenin yazım işlemini gerçekleştirmiştir.

#### CONFLICT OF INTEREST (ÇIKAR ÇATIŞMASI)

There is no conflict of interest in this study.

Bu çalışmada herhangi bir çıkar çatışması yoktur.

#### REFERENCES (KAYNAKLAR)

- [1] Y. Kaya, Journal of Polytechnic 21, 597 (2018).
- [2] E. Celasun, Heat Treatment and Welding of S355J2 Steel with Different Submerged Arc Welding Wires and Investigation of Their Effect on Weldability, Institute of Science and Technology, 2012.
- [3] H. F. Çapın, The Welding of S235 JR Non-Alloyed Steel Pipes with Orbital Welding Equipment at Vertical Position and the Optimization of the Application, Institute of Science and Technology, 2014.
- [4] S. Anik, Gedik Education Foundation Welding Technology Education Research and Inspection Institute (1991).
- [5] D. Yildirim, The Examination of Weldability of 2205 Duplex Stainless Steel and S355J2 Structural Steel, Institute of Science and Technology, 2018.
- [6] İ. Ertürk, T. Durukan, and B. Şentürk, in Xth Welding Technology National Congress and Exhibition (2017).
- [7] B. Eleman, Comparison of Macrostructure and Mechanical Properties of Welding Seams as a Result of S355 Quality Steel Welded by New Generation (Inverter) and Traditional MIG/MAG Welding Machines, Yıldız Technical University, 2022.
- [8] B. Yu, Z. Chen, P. Wang, and X. Song, Journal of Constructional Steel Research 205, 107878 (2023).
- [9] P. Zhao, B. Yu, P. Wang, Y. Liu, and X. Song, Materials 16, (2023).
- [10] Z. Zhu, X. Ma, P. Jiang, G. Mi, and C. Wang, Journal of Materials Research and Technology 10, 960 (2021).
- [11] S. A. David, S. S. Babu, and J. M. Vitek, JOM 55, 14 (2003).
- [12] M. Li, Y. He, and G. Sun, Materials & Design 25, 355 (2004).
- [13] M. Eroğlu, M. Aksoy, and N. Orhan, Materials Science and Engineering: A 269, 59 (1999).
- [14] E. Gharibshahiyan, A. H. Raouf, N. Parvin, and M. Rahimian, Materials & Design 32, 2042 (2011).
- [15] R. Yan, K. Mela, F. Yang, H. El Bamby, & M. Veljkovic, Thin-Walled Structures, 184, 110479 (2023).

- [16] R. Kaçar and K. Kökemli, *Materials & Design* 26, 508 (2005).
- [17] S. Mehra, P. Dhanda, R. Khanna, N. S. Goyat, & S. Verma. *International Journal of Scientific & Engineering Research*, 3(11), 1-6 (2012).
- [18] O. Tuncel and H. Aydin, *Materials Science* 26, 173 (2020).
- [19] K. Borko, B. Hadzima, and F. Pastorek, *Periodica Polytechnica Transportation Engineering* 47, 342 (2019).
- [20] H. Lgaz, K. Subrahmanya Bhat, R. Salghi, Shubhalaxmi, S. Jodeh, M. Algarra, B. Hammouti, I. H. Ali, and A. Essamri, *Journal of Molecular Liquids* 238, 71 (2017).

ERKEN GÖRÜNÜM